*Physiol. Res. 67 (Suppl. 3): S543-S550, 2018*

# Expression Profiling of *Nme7* Interactome in Experimental Models of Metabolic Syndrome

**L. ŠEDOVÁ[1,2], E. ŠKOLNÍKOVÁ[1,2], M. HODÚLOVÁ[2], J. VČELÁK[3], O. ŠEDA[2], B. BENDLOVÁ[3]**

[1]Laboratory of Transgenic Models of Diseases, Division BIOCEV, Institute of Molecular Genetics of the Czech Academy of Sciences, Vestec, Czech Republic, [2]Institute of Biology and Medical Genetics, First Faculty of Medicine, Charles University, Prague, Czech Republic, [3]Department of Molecular Endocrinology, Institute of Endocrinology, Prague, Czech Republic

Received August 24, 2018
Accepted September 11, 2018

**Summary**

Nucleoside diphosphate kinase 7, non-metastatic cells 7 (NME7) is an acknowledged member of ciliome and is involved in the biogenesis or function of cilia. As obesity and diabetes are common in several ciliopathies, we aimed to analyze changes of gene expression within *Nme7* interactome in genetically designed rat models of metabolic syndrome. We assessed the liver transcriptome by Affymetrix microarrays in adult males of 14 PXO recombinant inbred rat strains and their two progenitor strains, SHR-*Lx* and BXH2. In the strains with the lowest expression of *Nme7*, we have identified significant enrichment of transcripts belonging to *Nme7* interactome. In the subsequent network analysis, we have identified three major upstream regulators – *Hnf4a*, *Ppara* and *Nr1h4* and liver steatosis (p=0.0001) and liver necrosis/cell death (apoptosis of liver cells, p=0.0003) among the most enriched Tox categories. The mechanistic network reaching the top score showed substantial overlap with Assembly of non-motile cilium and Glucose metabolism disorder gene lists. In summary, we show in a genetic model of metabolic syndrome that rat strains with the lowest expression of *Nme7* present gene expression shifts of *Nme7* interactome that are perturbing networks relevant for carbohydrate and lipid metabolism as well as ciliogenesis.

**Key words**

Metabolic syndrome • Transcriptomics • Recombinant inbred strains • Ciliopathy

**Corresponding author**

L. Šedová, Laboratory of Transgenic Models of Diseases, Division BIOCEV, Institute of Molecular Genetics of the Czech Academy of Sciences, v.v.i., 252 42 Vestec, Czech Republic. E-mail: lucie.sedova@img.cas.cz

## Introduction

NME7 (nucleoside diphosphate kinase 7, non-metastatic cells 7) is a member of the conserved NME/NDK family of multifunctional enzymes that mostly act as nucleoside-diphosphate kinases and protein histidine kinases. Although the NME7 gene contains two putative kinase domains, it does not seem to possess a nucleoside-diphosphate kinase activity (Liu *et al.* 2014).

The NME7 transcript and protein are detected in majority of tissues. At the subcellular level, the NME7 shows mainly centrosomal localization. The centrosomal content of NME7 is dependent on the phase of the cell cycle: the NME 7 level at the centrosome was lowest in early G1 phase and highest in metaphase, and during mitosis, NME7 was also detected at mitotic spindles and in the midbody during cytokinesis (Liu *et al.* 2014).

NME7 is implicated in the regulation of the microtubule-nucleating activity of the γTuRC in centrosomes. At centrosomes, γ-tubulin participates in centriole duplication and primary cilium assembly, in addition to performing microtubule-nucleating and microtubule-organizing functions (Mikule *et al.* 2007, Liu *et al.* 2014).

The effect of NME7 depletion on cilia number, length, function and ciliary cargo transport (Lai *et al.* 2011) has been studied as NME7 is an acknowledged member of ciliome (Ostrowski *et al.* 2002). The study results suggest that by being localized at the centrosome, the NME7 is suitably positioned to possibly regulate specific ciliary cargoes either at the ciliary gate or from the Golgi (Lai *et al.* 2011).

Possible role of NME7 in the development of ciliopathies was tested in the *Nme7*$^{-/-}$ mice knockout model. *Nme7*$^{-/-}$ mice were viable and fertile and did not differ in gross appearance from wild-type littermates. As all *Nme7*$^{-/-}$ mice exhibited mild to moderate hydrocephalus and 50 % of *Nme7*$^{-/-}$ mice had situs inversus, the NME7 protein is very likely involved in the biogenesis or function of motile cilia (Vogel *et al.* 2010). Obesity and diabetes are common features of several ciliopathies including Alstrom and Bardet-Biedl syndromes. The potential connection between glucose metabolism and proper cilia function was recently reviewed in detail by Lodh *et al.* (2014). They concluded that "the emerging evidence suggests that disruption of glucose regulation in ciliopathies — and potentially in more common diseases — may be directly linked to the regulation of signaling that is highly dependent on cilia and is critical to proper pancreatic morphogenesis" (Lodh *et al.* 2014). While the causal mechanistic relation between NME7 and metabolic disturbances through cilia dysfunction remains to be established, it represents a preliminary plausible link. Furthermore, the recently revealed functional connection between (pro)renin receptor PRR (ATP6AP2) and NME7 may extend beyond the cell cycle control (Wanka *et al.* 2017) as it was previously shown that PRR is involved in regulation of body weight, fat mass and insulin resistance (Shamansurova *et al.* 2016, Ahmed *et al.* 2011).

As the analysis of multifaceted relationships underlying complex traits is complicated by numerous factors inherent to general human population studies, genetically designed models are frequently used. In particular, mouse and rat models have been seminal for genetic and pathophysiological studies of metabolic syndrome and its ecogenomic (nutrigenomic, pharmacogenomic, epigenomic, metagenomic etc.) aspects (Civelek and Lusis 2014, Poledne and Jurcikova-Novotna 2017, Kunes *et al.* 2015). Derived from the reference rat panel for genetic dissection of cardiovascular complex traits, the HXB BXH recombinant inbred strain panel (Pravenec *et al.* 1989), the set of PXO recombinant inbred rat strains (Kemlink *et al.* 2003, Hodulova *et al.* 2014) is a genetically fixed system with segregating alleles of two highly inbred models of metabolic syndrome, the spontaneously hypertensive rat (SHR) (Coan *et al.* 2017) and the polydactylous rat PD/Cub (Sedova *et al.* 2000, Seda *et al.* 2002), together with normotensive and normolipidemic Brown Norway (BN/Cub) strain. Also, while single gene mutants often provide important insights into the gene function and involvement in particular signaling or metabolic pathway, the genomic architecture of most complex traits involves modular networks of genes (Civelek and Lusis 2014, Seda *et al.* 2017b), where both more subtle genetic variation and even effects of genomic background may lead to substantial disruptions of crucial mechanisms and shift the balance between the health and disease. In our study, we aimed to test the expression profile of *Nme7* and its interactome in the genetically defined model set of metabolic syndrome.

## Methods

All experiments were performed in agreement with the Animal Protection Law of the Czech Republic (311/1997) which follows the European Community Council recommendations for the use of laboratory animals 86/609/ECC and were approved by the Ethical Committee of the First Faculty of Medicine of the Charles University.

*Liver tissue samples*

The samples of livers obtained in a previous study of PXO strains (Hodulova *et al.* 2014) were utilized in the current study. Used rat strains are cataloged in Rat Genome Database (RGD) (Shimoyama *et al.* 2016). Four samples per strain were analyzed from adult (4-months old) male rats of 14 PXO strains (PXO1/Cub, RGD ID 2307138; PXO2/Cub, RGD ID 2307356; PXO3-1/Cub, RGD ID 2307355; PXO3-2/Cub, RGD ID 2307116; PXO4/Cub, RGD ID 2307135; PXO5-1/Cub, RGD ID 2307128; PXO5-2/Cub, RGD ID 2307117; PXO6-1/Cub, RGD ID 2307137; PXO6-2/Cub, RGD ID 2307125; PXO6-3/Cub, RGD ID 2307130; PXO7/Cub, RGD ID 2307119; PXO8-1/Cub, RGD ID 2307122; PXO8-2/Cub, RGD ID 2307131; PXO10/Cub, RGD ID 2307132) as well as the progenitor strains SHR-*Lx* (RGD ID 61106) and BXH2/Cub (BXH2 hereafter, RGD ID 2307121). All abovementioned strains were originally derived and kept since at the animal facility of Institute of Biology and

Medical Genetics, Fist Faculty of Medicine, Charles University in Prague.

*Genotype comparison*

The genotype comparison of PXO strains was performed *in silico* using previously ascertained >1,000 microsatellite markers (Kemlink *et al.* 2003) (Hodulova *et al.* 2014) and >20,000 single nucleotide polymorphisms made available by STAR Consortium (2008).

*Liver transcriptome assessment*

Total RNA was isolated from liver tissue (RNeasy Mini Kit, Qiagen, Hilden, Germany). The quality and integrity of the total RNA was evaluated on Agilent 2100 Bioanalyzer system (Agilent, Palo Alto, CA, USA). Only samples with RNA Integrity Number (RIN) >8.0 were utilized in further steps of the protocol. Microarray experiments were performed using the Rat Gene 2.1 ST Array Strip in quadruplicate per strain. The hybridization procedure was performed using the Affymetrix GeneAtlas® system according to manufacturer's instructions. The quality control of the chips was performed using Transcriptome Analysis Console 4.0 (Life Technologies, Carlsbad, CA, USA). Partek Genomics Suite 6.6 (Partek, St. Louis, Missouri, USA) was used for subsequent data analysis. After applying quality filters and data normalization by Robust Multichip Average (RMA) algorithm, the set of obtained differentially expressed probesets was filtered by false discovery rate (FDR<0.05) method implemented in Partek Genomics Suite 6.6 (Partek, St. Louis, Missouri, USA).

*Network analyses*

Transcriptomic data were then processed by standardized sequence of analyses (hierarchical clustering and principal component analysis, gene ontology, gene set enrichment, 'Upstream Regulator Analysis', 'Mechanistic Networks', 'Causal Network Analysis' and 'Downstream Effects Analysis') using Ingenuity Pathway Analysis as described previously (Seda *et al.* 2017a).

*Statistics*

To compare the expression of *Nme7* among the PXO and progenitor strains, one-way ANOVA with Strain as a major factor followed by Tukey-Kramer HSD *post hoc* test was used. Fisher's exact test was employed to test the hypothesis of enrichment of focus molecules in the overlap of gene sets.

## Results

*Nme7 expression in PXO recombinant inbred set*

The expression of *Nme7* in the PXO strains showed a pattern of transgressive variation in relation to their progenitors as shown in Figure 1. The overall difference in expression among tested strains was statistically significant (ANOVA p=3.12E-05) but when we performed series of pairwise comparisons of progenitor strains with the individual PXO strains, only PXO6-2 strain showed decreased expression of *Nme7* compared both to BXH2 (p=0.047) and SHR-*Lx* (p=0.037) after adjustment for multiple comparisons. All three PXO6 strains clustered in the left-hand side of the distribution and showed lower expression when compared to PXO3-2 strain (p=0.046, 0.0006 and 0.01 for PXO6-1, PXO6-2 and PXO6-3, respectively). PXO6-2 showed also lower expression compared to PXO10 (p=0.006), PXO4 (p=0.007) and PXO3-1 (p=0.028) strains.

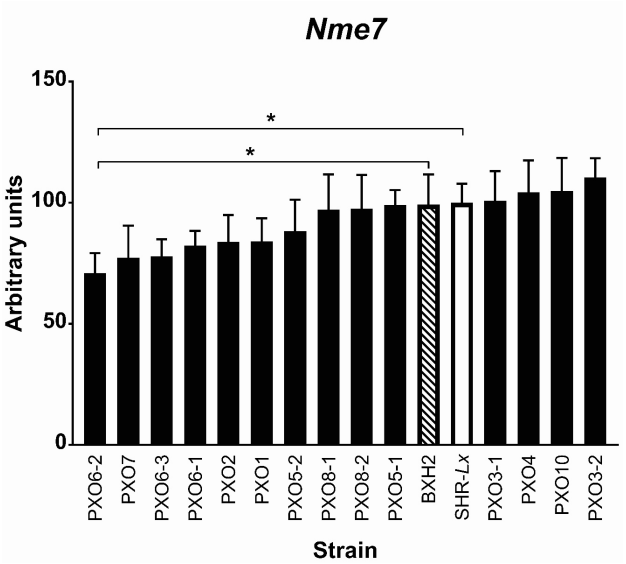


**Fig. 1**. Expression profile of *Nme7* in livers of PXO recombinant inbred strains and their progenitors. The expression is shown in arbitrary units relative to expression of SHR-*Lx*, which is set to 100. Only significant differences between progenitors (BXH2 – striped bar, SHR-*Lx* – white bar) and individual PXO strains are shown. The p-values reflect Tukey-Kramer HSD *post hoc* test of one-way ANOVA with Strain as a major factor: *p<0.05.

*Genomic comparison of PXO6 strains*

Given their co-occurrence at the low extreme of *Nme7* expression distribution, we compared the genomic profiles of PXO6-1, PXO6-2 and PXO6-3 strains. Based on the data from over 21,000 SNP and microsatellite markers, we have established that PXO6-2 and PXO6-3

display the highest genetic similarity with only 0.703 % differing markers while PXO6-1 showed 3.540 % and 4.132 % difference from PXO6-2 and PXO6-3, respectively. The segments distinguishing PXO6-1 from the other two strains are located on chromosomes 3, 5, 9, 12 and 16, while PXO6-3 differs from PXO6-2 and PXO6-1 in a segment of chromosome 4. As all three strains are close on both genomic level and with regard to *Nme7* expression, we performed further transcriptome analyses using these three strains in comparison to SHR-*Lx*, the source of *Nme7* variant in PXO strain set.

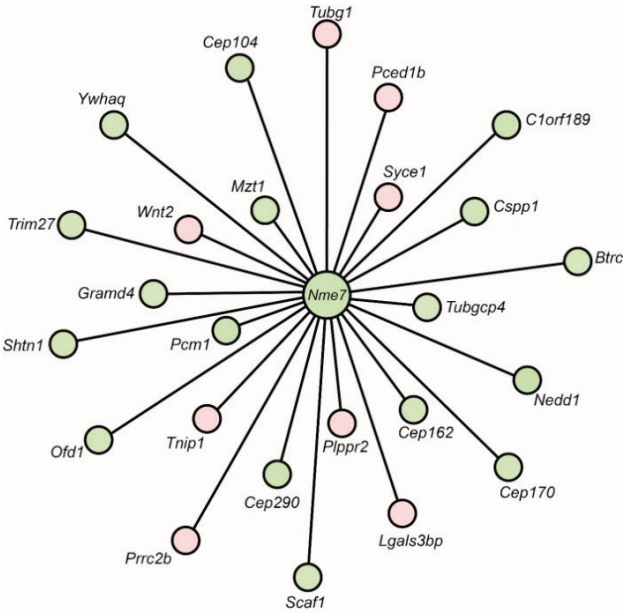


**Fig. 2**. Overlap between *Nme7* interactome and significant differences between liver transcriptomes of male rats of SHR-*Lx* progenitor and PXO6 strains. The shades of green and red depict the level of significantly lower or higher expression in the PXO6 strains compared to SHR-*Lx*, respectively. *Btrc* – beta-transducin repeat containing E3 ubiquitin protein ligase, *C1orf189* – chromosome 1 open reading frame 189, *Cep104* – centrosomal protein 104, *Cep162* – centrosomal protein 162, *Cep170* – centrosomal protein 170, *Cep290* centrosomal protein 290, *Cspp1* – centrosome and spindle pole associated protein 1, *Gramd4* – GRAM domain containing 4, *Lgals3bp* – galectin 3 binding protein, *Mzt1* – mitotic spindle organizing protein 1, *Nedd1* – neural precursor cell expressed, developmentally down-regulated 1, *Ofd1* – centriole and centriolar satellite protein, *Pced1b* – PC-esterase domain containing 1B, *Pcm1* – pericentriolar material 1, *Plppr2* – phospholipid phosphatase related 2, *Prrc2b* – proline rich coiled-coil 2B, *Scaf1* – SR-related CTD associated factor 1, *Shtn1* – shootin 1, *Syce1* – synaptonemal complex central element protein 1, *Tnip1* – TNFAIP3 interacting protein 1, *Trim27* – tripartite motif containing 27, *Tubg1* – tubulin gamma 1, *Tubgcp4* – tubulin gamma complex associated protein 4, *Wnt2* – Wnt family member 2, *Ywhaq* – tyrosine 3-monooxygenase/tryptophan 5-monooxygenase activation protein theta.

*Nme7 interactome vs. PXO6 liver transcriptome*

Utilizing Ingenuity Knowledge Base and literature search, we ascertained a set of 109 entities (protein-coding genes, microRNAs) that were shown to interact with *Nme7* on a molecular level. Then, we performed liver transcriptome comparison of SHR-*Lx* with PXO6-1, PXO6-2 and PXO6-3 strains. After multiple-testing correction by false discovery rate (FDR<0.05), 1,544 transcripts showed significantly different expression in all three PXO6 strains compared to SHR-*Lx.* An overlap between *Nme7* interactome revealed 26 genes that were differentially expressed corresponding to significant ($p<0.00001$, Fisher's exact test) enrichment of *Nme7* interactome member entities in the differentially expressed transcripts between PXO6 and SHR-*Lx* (Fig. 2). Except for *Pced1b*, which is of SHR origin in PXO6-1 and of BXH2 origin in PXO6-2 and PXO6-3, the 25 other genes are of the same origin in all three strains (*C1orf189*, *Cep104*, *Cep170*, *Cep290*, *Gramd4, Nedd1*, *Pcm1* and *Wnt2* from SHR-*Lx* and the remaining 16 genes from BXH2).

*Enrichment analysis and mechanistic network construction*

We combined the directional information comprising the 1,544 transcripts differentially expressed in PXO6-1, PXO6-2 and PXO6-3 strains compared to SHR-*Lx* with available data on experimentally observed cause-effect relationships that relate to expression, transcription, activation, molecular modification and transport utilizing causal analytics algorithms including Upstream Regulator Analysis, Causal Networks Analysis and Mechanistic Networks as implemented in Ingenuity Pathway Analysis software (Kramer *et al.* 2014). The top upstream regulators, i.e. molecules upstream of the differentially expressed genes that potentially explain the observed expression changes, were hepatocyte nuclear factor 4, alpha (*Hnf4a*, p=1.15E-11), peroxisome proliferator activated receptor alpha (*Ppara*, p=1.28E-07) and nuclear receptor subfamily 1, group H, member 4 (*Nr1h4,* p=2.34E-06). The significantly enriched "Tox"categories after Benjamini-Hochberg correction for multiple comparisons were liver steatosis (p=0.0001) and liver necrosis/cell death (apoptosis of liver cells, p=0.0003). The mechanistic network reaching the highest score (reflecting the network's degree of relevance to the network eligible set of 1,544 transcripts based on hypergeometric distribution and right-tailed Fisher's exact test) is shown in Figure 3. Next, we have assessed the enrichment of disease and functional categories within this mechanistic network, revealing two most enriched terms, Assembly of non-motile cilium and Glucose metabolism disorder.

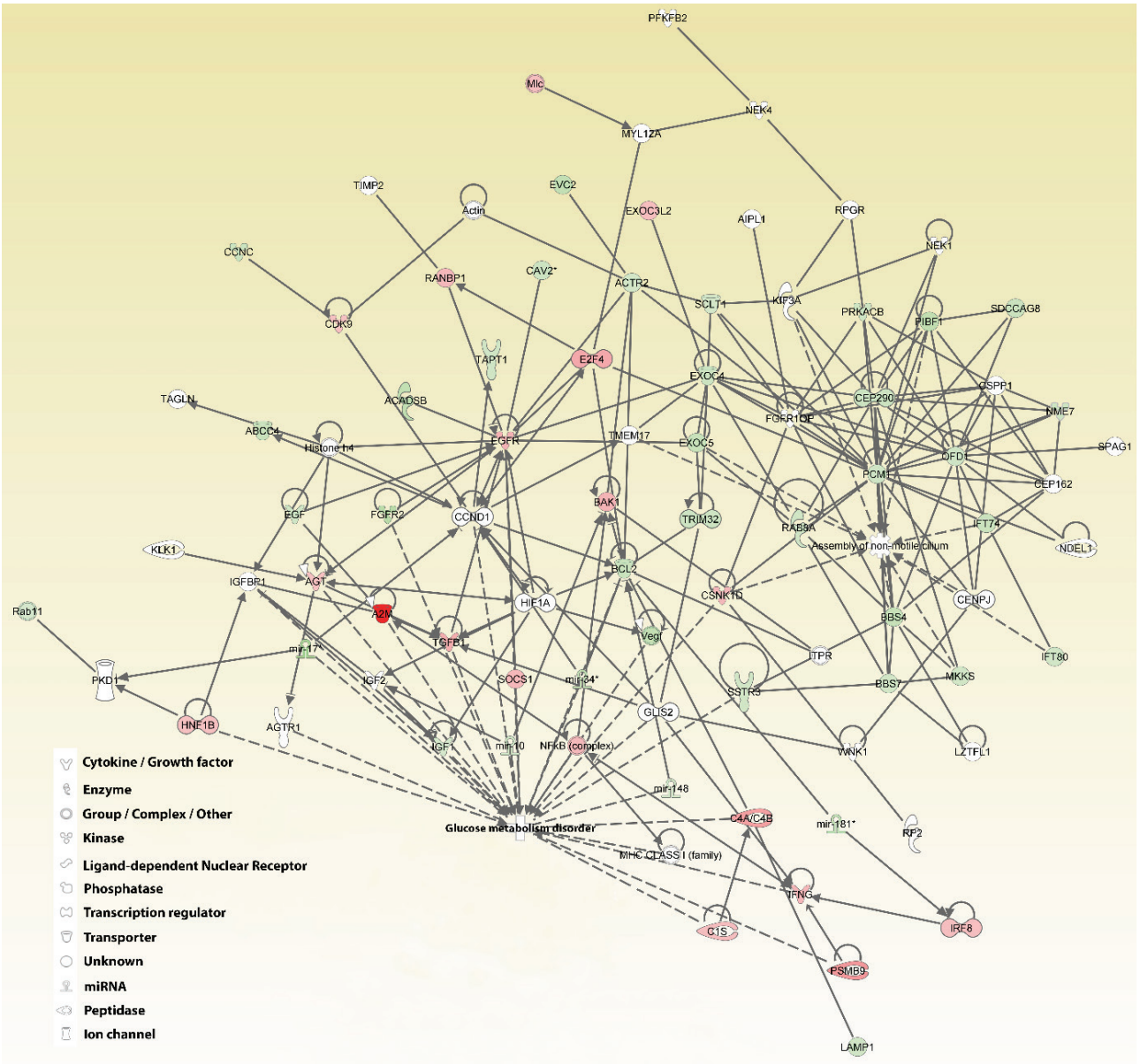


**Fig. 3.** Mechanistic network derived from set of differentially expressed genes in PXO6-1, PXO6-2 and PXO6-3 strains compared with SHR-*Lx* progenitor. Mechanistic network with highest score derived from the set of genes that were significantly differentially expressed in all three PXO6 strains when compared to SHR-*Lx* progenitor strain. The network reaching the highest score based on Ingenuity Pathway Analysis is shown with disease and function terms showing highest overlap score (Assembly of non-motile cilium, glucose metabolic disorder). The shades of green and red depict the level of significantly lower or higher expression in the PXO6-2 (PXO strain with the lowest *Nme7* expression) vs. SHR-*Lx*. Entities with white symbols form part of the network but their expression did not differ between PXO6-2 and SHR-*Lx*. The scheme was generated using Ingenuity Pathway Analysis (Qiagen, Hilden, Germany). The abbreviations of gene names are used according to HUGO Gene Nomenclature Committee guidelines (https://www.genenames.org/).

## Discussion

In this study, we show in a genetically designed model set of metabolic syndrome that rat strains with the lowest expression of *Nme7* present gene expression shifts of *Nme7* interactome that are perturbing networks relevant for carbohydrate and lipid metabolism as well as ciliogenesis. This observation is consistent with our previous findings that PXO6 strains display lower body weight and relative weight of retroperitoneal fat as well as lower cholesterol concentrations in chylomicron, very low-density lipoprotein (VLDL), low-density lipoprotein (LDL-C) fractions and higher high-density lipoprotein (HDL) cholesterol compared to SHR-*Lx* progenitor (Hodulova *et al.* 2014). All the identified upstream regulators (*Hnf4a*, *Ppara* and *Nr1h4*) belong to richly evidenced major nodes orchestrating lipid and carbohydrate metabolism (Hayhurst *et al.* 2001, Seda and Sedova 2007, Han 2018). Interestingly, the involvement of PPARA and NR1H4 in autophagy-ciliogenesis axis

was recently demonstrated, providing a potential mechanistic link between the two seemingly unrelated processes (Liu *et al.* 2018). While the crucial role of NME7 in primary cilium assembly and function is well known, the connection to metabolic syndrome-related disturbances was not reported so far. Mouse models with genetically engineered *Nme7* deficiency (Vogel *et al.* 2010, Vogel *et al.* 2012) and the human cases of sporadic mutations leading to severe damage to the protein product (Reish *et al.* 2016) all develop substantial morphological and functional consequences including situs inversus totalis and hydrocephalus. Compared to these loss-of-function mutations, a subtler variation in NME7/Nme7 gene present in general human population or specific experimental models may produce distinct effects, either directly through primary cilium dysfunction (as the majority of differentially expressed *Nme7* interactome genes in our study are connected to centrosome assembly) or through more likely mechanism of perturbed signaling pathways and networks. In genome-wide association studies, association of SNPs within *Nme7* gene to venous thromboembolism (consisting of deep vein thrombosis and its complication, pulmonary embolism) (Heit *et al.* 2012) and D-dimer levels (Smith *et al.* 2011) were reported. Also, the T allele of rs1138486 was associated to QT interval length in almost 16,000 people of Hispanic/Latino descent (Mendez-Giraldez *et al.* 2017). Most recently, rs12753816 was shown to be associated to coronary artery disease (van der Harst and Verweij 2018). However, in some of the mentioned studies strong linkage disequilibrium with Factor V Leiden mutation is mentioned as a potential confounder.

There are several inherent limitations of our study. First, the observations are made only at the level of transcriptome and need to be confirmed at protein and functional levels in further studies to provide true mechanistic links underlying the observed shifts in perturbed networks. Second, despite consistence of physiological measures and the expression and network-level data, all were acquired in a single model system restricted to male animals with specific genomic makeup. Validation in other models and particularly in human studies is necessary to corroborate the potential clinical impact of the *Nme7* variation. In conclusion, results presented in this study suggest a role of Nme7 beyond ciliogenesis with potential impact on metabolic syndrome features.

## Conflict of Interest

There is no conflict of interest.

## Acknowledgements

This work was supported by Czech Science Foundation Project 17-13491S and Charles University in Prague (Progres Q25/LF1, SVV 260367) and by Ministry of Health CR (DRO 00023761).

## References

AHMED BA, SEDA O, LAVOIE JL: (Pro)renin receptor as a new drug target. *Curr Pharm Des* **17**: 3611-3621, 2011.

CIVELEK M, LUSIS AJ: Systems genetics approaches to understand complex traits. *Nat Rev Genet* **15**: 34-48, 2014.

COAN PM, HUMMEL O, GARCIA DIAZ A, BARRIER M, ALFAZEMA N, NORSWORTHY PJ, PRAVENEC M, PETRETTO E, HUBNER N, AITMAN TJ: Genetic, physiological and comparative genomic studies of hypertension and insulin resistance in the spontaneously hypertensive rat. *Dis Model Mech* **10**: 297-306, 2017.

HAN CY: Update on FXR biology: promising therapeutic target? *Int J Mol Sci* **19**: E2069, 2018.

HAYHURST GP, LEE YH, LAMBERT G, WARD JM, GONZALEZ FJ: Hepatocyte nuclear factor 4alpha (nuclear receptor 2A1) is essential for maintenance of hepatic gene expression and lipid homeostasis. *Mol Cell Biol* **21**: 1393-1403, 2001.

HEIT JA, ARMASU SM, ASMANN YW, CUNNINGHAM JM, MATSUMOTO ME, PETTERSON TM, DE ANDRADE M: A genome-wide association study of venous thromboembolism identifies risk variants in chromosomes 1q24.2 and 9q. *J Thromb Haemost* **10**: 1521-1531, 2012.

HODULOVA M, SEDOVA L, KRENOVA D, LISKA F, KRUPKOVA M, KAZDOVA L, TREMBLAY J, HAMET P, KREN V, SEDA O: Genomic determinants of triglyceride and cholesterol distribution into lipoprotein fractions in the rat. *PLoS One* **9**: e109983, 2014.

KEMLINK D, JERABKOVA V, JANKU M, KRENOVA D, KREN V: PXO set of recombinant inbred strains of the rat: a new strain distribution pattern containing 448 markers. *Folia Biol (Praha)* **49**: 165-176, 2003.

KRAMER A, GREEN J, POLLARD J JR, TUGENDREICH S: Causal analysis approaches in Ingenuity Pathway Analysis. *Bioinformatics* **30**: 523-530, 2014.

KUNES J, VANECKOVA I, MIKULASKOVA B, BEHULIAK M, MALETINSKA L, ZICHA J: Epigenetics and a new look on metabolic syndrome. *Physiol Res* **64**: 611-620, 2015.

LAI CK, GUPTA N, WEN X, RANGELL L, CHIH B, PETERSON AS, BAZAN JF, LI L, SCALES SJ: Functional characterization of putative cilia genes by high-content analysis. *Mol Biol Cell* **22**: 1104-1019, 2011.

LIU P, CHOI YK, QI RZ: NME7 is a functional component of the gamma-tubulin ring complex. *Mol Biol Cell* **25**: 2017-2025, 2014.

LIU ZQ, LEE JN, SON M, LIM JY, DUTTA RK, MAHARJAN Y, KWAK S, OH GT, BYUN K, CHOE SK, PARK R: Ciliogenesis is reciprocally regulated by PPARA and NR1H4/FXR through controlling autophagy in vitro and in vivo. *Autophagy* **14**: 1011-1027, 2018.

LODH S, O'HARE EA, ZAGHLOUL NA: Primary cilia in pancreatic development and disease. *Birth Defects Res C Embryo Today* **102**: 139-158, 2014.

MENDEZ-GIRALDEZ R, GOGARTEN SM, BELOW JE, YAO J, SEYERLE AA, HIGHLAND HM, KOOPERBERG C, SOLIMAN EZ, ROTTER JI, KERR KF, RYCKMAN KK, TAYLOR KD, PETTY LE, SHAH SJ, CONOMOS MP, SOTOODEHNIA N, CHENG S, HECKBERT SR, SOFER T, GUO X, WHITSEL EA, LIN HJ, HANIS CL, LAURIE CC, AVERY CL: GWAS of the electrocardiographic QT interval in Hispanics/Latinos generalizes previously identified loci and identifies population-specific signals. *Sci Rep* **7**: 17075, 2017.

MIKULE K, DELAVAL B, KALDIS P, JURCYZK A, HERGERT P, DOXSEY S: Loss of centrosome integrity induces p38-p53-p21-dependent G1-S arrest. *Nat Cell Biol* **9**: 160-170, 2007.

OSTROWSKI LE, BLACKBURN K, RADDE KM, MOYER MB, SCHLATZER DM, MOSELEY A, BOUCHER RC: A proteomic analysis of human cilia: identification of novel components. *Mol Cell Proteomics* **1**: 451-465, 2002.

POLEDNE R, JURCIKOVA-NOVOTNA L: Experimental models of hyperlipoproteinemia and atherosclerosis. *Physiol Res* **66** (Suppl 1): S69-S75, 2017.

PRAVENEC M, KLIR P, KREN V, ZICHA J, KUNES J: An analysis of spontaneous hypertension in spontaneously hypertensive rats by means of new recombinant inbred strains. *J Hypertens* **7**: 217-221, 1989.

REISH O, ASPIT L, ZOUELLA A, ROTH Y, POLAK-CHARCON S, BABOUSHKIN T, BENYAMINI L, SCHEETZ TE, MUSSAFFI H, SHEFFIELD VC, PARVARI R: A homozygous Nme7 mutation is associated with situs inversus totalis. *Hum Mutat* **37**: 727-731, 2016.

SEDA O, SEDOVA L: Peroxisome proliferator-activated receptors as molecular targets in relation to obesity and type 2 diabetes. *Pharmacogenomics* **8**: 587-596, 2007.

SEDA O, KAZDOVA L, KRENOVA D, KREN V: Rosiglitazone improves insulin resistance, lipid profile and promotes adiposity in a genetic model of metabolic syndrome X. *Folia Biol (Praha)* **48**: 237-241, 2002.

SEDA O, LISKA F, PRAVENEC M, VERNEROVA Z, KAZDOVA L, KRENOVA D, ZIDEK V, SEDOVA L, KRUPKOVA M, KREN V: Connexin 50 mutation lowers blood pressure in spontaneously hypertensive rat. *Physiol Res* **66**: 15-28, 2017a.

SEDA O, SEDOVA L, VCELAK J, VANKOVA M, LISKA F, BENDLOVA B: ZBTB16 and metabolic syndrome: a network perspective. *Physiol Res* **66** (Suppl 3): S357-S365, 2017b.

SEDOVA L, KAZDOVA L, SEDA O, KRENOVA D, KREN V: Rat inbred PD/cub strain as a model of dyslipidemia and insulin resistance. *Folia Biol (Praha)* **46**: 99-106, 2000.

SHAMANSUROVA Z, TAN P, AHMED B, PEPIN E, SEDA O, LAVOIE JL: Adipose tissue (P)RR regulates insulin sensitivity, fat mass and body weight. *Mol Metab* **5**: 959-969, 2016.

SHIMOYAMA M, LAULEDERKIND SJ, DE PONS J, NIGAM R, SMITH JR, TUTAJ M, PETRI V, HAYMAN GT, WANG SJ, GHIASVAND O, THOTA J, DWINELL MR: Exploring human disease using the Rat Genome Database. *Dis Model Mech* **9**: 1089-1095, 2016.

SMITH NL, HUFFMAN JE, STRACHAN DP, HUANG J, DEHGHAN A, TROMPET S, LOPEZ LM, SHIN SY, BAUMERT J, VITART V, BIS JC, WILD SH, RUMLEY A, YANG Q, UITTERLINDEN AG, STOTT DJ, DAVIES G, CARTER AM, THORAND B, POLASEK O, MCKNIGHT B, CAMPBELL H, RUDNICKA AR, CHEN MH, BUCKLEY BM, HARRIS SE, PETERS A, PULANIC D, LUMLEY T, DE CRAEN AJ, LIEWALD DC, GIEGER C, CAMPBELL S, FORD I, GOW AJ, LUCIANO M, PORTEOUS DJ, GUO X, SATTAR N, TENESA A, CUSHMAN M, SLAGBOOM PE, VISSCHER PM, SPECTOR TD, ILLIG T, RUDAN I, BOVILL EG, WRIGHT AF, MCARDLE WL, TOFLER G, HOFMAN A, WESTENDORP RG, STARR JM, GRANT PJ, KARAKAS M, HASTIE ND, PSATY BM, WILSON JF, LOWE GD, O'DONNELL CJ, WITTEMAN JC, JUKEMA JW, DEARY IJ, SORANZO N, KOENIG W, HAYWARD C: Genetic predictors of fibrin D-dimer levels in healthy adults. *Circulation* **123**: 1864-1872, 2011.

STAR CONSORTIUM, SAAR K, BECK A, BIHOREAU MT, BIRNEY E, BROCKLEBANK D, CHEN Y, CUPPEN E, DEMONCHY S, DOPAZO J, FLICEK P, FOGLIO M, FUJIYAMA A, GUT IG, GAUGUIER D, GUIGO R, GURYEV V, HEINIG M, HUMMEL O, JAHN N, KLAGES S, KREN V, KUBE M, KUHL H, KURAMOTO T, KUROKI Y, LECHNER D, LEE YA, LOPEZ-BIGAS N, LATHROP GM, MASHIMO T, MEDINA I, MOTT R, PATONE G, PERRIER-CORNET JA, PLATZER M, PRAVENEC M, REINHARDT R, SAKAKI Y, SCHILHABEL M, SCHULZ H, SERIKAWA T, SHIKHAGAIE M, TATSUMOTO S, TAUDIEN S, TOYODA A, VOIGT B, ZELENIKA D, ZIMDAHL H, HUBNER N: SNP and haplotype mapping for genetic analysis in the rat. *Nat Genet* **40**: 560-566, 2008.

VAN DER HARST P, VERWEIJ N: Identification of 64 novel genetic loci provides an expanded view on the genetic architecture of coronary artery disease. *Circ Res* **122**: 433-443, 2018.

VOGEL P, READ R, HANSEN GM, FREAY LC, ZAMBROWICZ BP, SANDS AT: Situs inversus in Dpcd/Poll-/-, Nme7-/-, and Pkd1l1-/- mice. *Vet Pathol* **47**: 120-131, 2010.

VOGEL P, READ RW, HANSEN GM, PAYNE BJ, SMALL D, SANDS AT, ZAMBROWICZ BP: Congenital hydrocephalus in genetically engineered mice. *Vet Pathol* **49**: 166-181, 2012.

WANKA H, LUTZE P, STAAR D, PETERS B, MORCH A, VOGEL L, CHILUKOTI RK, HOMUTH G, SCZODROK J, BAUMGEN I, PETERS J: (Pro)renin receptor (ATP6AP2) depletion arrests As4.1 cells in the G0/G1 phase thereby increasing formation of primary cilia. *J Cell Mol Med* **21**: 1394-1410, 2017.